Doping-Induced Change of Superconducting Gap Anisotropy in $Bi_2Sr_2Ca_1Cu_2O_{8+\delta}$

R. J. Kelley, C. Quitmann, M. Onellion,* H. Berger, P. Almeras, G. Margaritondo

High-resolution angle-resolved photoemission measurements were performed on single crystals of $Bi_2Sr_2Ca_1Cu_2O_{8+\delta}$ with different oxygen stoichiometries. The data establish that the gap anisotropy (ratio of the gap along Γ-M to the gap along Γ-X) can be reversibly changed from ~20:1 (optimal or underdoped) to ~2:1 (overdoped). Differences in sample doping explain the conflicting reports on gap anisotropy in the literature. Possible effects of this change in gap anisotropy on the symmetry of the order parameter are discussed. There remains some ambiguity as to the relation between the order parameter and doping.

The symmetry of the order parameter in high-temperature superconductors is an extremely interesting, widely investigated, and controversial subject. A knowledge of the symmetry can be used to distinguish possible mechanisms responsible for the high superconducting transition temperatures in the cuprates. In our recent work (*1*, *2*), we developed the hypothesis that the controversy stems from previously unnoticed doping effects. In addition, several recent theoretical analyses (*3*–*5*) have argued, on different grounds, that the order parameter has two components with relative weights that change with stoichiometry.

Basically, the controversy concerns experimental evidence in support of several possible symmetries of the order parameter. In superconductivity, researchers use the terms "*s*-wave" and "conventional" order parameter to mean that the symmetry of the order parameter is the same as that of the crystal lattice. Low-temperature superconductors are conventional and, at low temperatures, exhibit no nodes in the superconducting gap anywhere on the Fermi surface.

Some of the tunneling data on $YBa_2Cu_3O_{7-x}$ support an *s*-wave symmetry in accord with Bardeen-Cooper-Schrieffer (BCS) theory, with no nodes in the gap (*6*). Other tunneling data (*7*), penetration length data (*8*), and some phase-sensitive work (*9*) on $YBa_2Cu_3O_{7-x}$ support a *d*-wave symmetry with nodes in certain directions. Some of the angle-resolved photoemission data on $Bi_2Sr_2CaCu_2O_{8+x}$ also support a *d*-wave symmetry (*10*, *11*), or more conservatively, suggest that the order parameter must be at least partly unconventional (*12*–*14*). In addition, several authors have proposed modified *s*-wave symmetries, such as extended *s*-wave (*11*, *15*), that have nodes but exhibit the symmetry of the lattice. Finally, there have been proposals that the gap symmetry includes two components, the relative weights of which change with stoichiometry (*3*, *5*, *16*). Unfortunately, experimental results by different reputable authors seemed to support conflicting symmetries, thus failing to provide a solid base for theory.

We performed high-resolution angle-resolved photoemission experiments on $Bi_2Sr_2Ca_1Cu_2O_{8+\delta}$ samples with different oxygen dopings. When samples are cooled below the superconducting transition temperature (T_c), a gap $\Delta(k)$ (dependent on momentum k) opens up at the Fermi surface in the single-particle photoemission excitation spectrum. Photoemission measures the magnitude and momentum dependence of the gap (the order parameter) but not the sign of the order parameter.

The interpretation of much of the previous experimental work has implicitly assumed that the gap symmetry is the same for all materials and stoichiometries. We initiated the present study to determine whether the gap anisotropy in $Bi_2Sr_2CaCu_2O_{8+x}$ was in fact invariant with respect to stoichiometry. We found that the gap along the Γ-X ($k_x = k_y$) direction changes dramatically (by at least a factor of 10) with the oxygen stoichiometry, whereas the gap near the M point is virtually unaffected (Γ-M is the k_x direction in reciprocal space, the Cu-O-Cu bond axis in real space). These results are consistent with a two-component order parameter (*3*, *5*, *16*); however, a modified *s*-wave order parameter (*11*, *15*) cannot be ruled out.

Single-crystal samples of $Bi_2Sr_2Ca_1Cu_2O_{8+\delta}$ were grown by the self-flux method (*17*). High-quality crystals as large as 2 cm by 1 cm were produced in this fashion. Our x-ray analysis showed that the samples were free of secondary phases to better than 2% (the limit of resolution). Selected crystals were overdoped by annealing in oxygen at 550°C for 4 days, and oxygen was removed from other crystals by annealing in argon at 700°C for 2 days. Samples were then measured by four-point resistivity or ac susceptibility. Argon-annealed samples had a T_c = 92 K (optimally doped); oxygen annealing produced a T_c = 85 K, with transition widths as narrow as 0.5 K (*18*) (measured by susceptibility for both types of samples).

The final test of sample quality was confirmed by in situ analysis. The samples were optically flat before cleaving, which was done at temperatures below 40 K. The surface quality was checked by both optical reflectivity and low-energy electron diffraction (LEED). The LEED provided a sensitive measure of surface order, an important point in retaining a well-defined photoelectron wave vector. If we obtained a well-ordered electron diffraction pattern at a kinetic energy of 25 eV or less, then the surface was considered to be of high quality.

Angle-resolved photoemission spectroscopy was performed at the Wisconsin Synchrotron Radiation Center in Stoughton, Wisconsin, with the 4-m normal incidence mono-

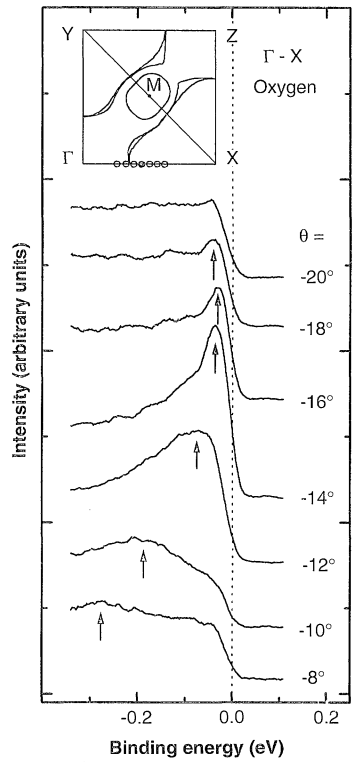

Fig. 1. A series of angle-resolved photoemission spectra of an overdoped sample (annealed in oxygen) for different azimuthal angles θ along the Γ-X direction (resolution, 50 meV; sample temperature, 20 K; photon energy, 21 eV). Arrows indicate the location of the dispersing quasi-particle state, referenced to the Fermi energy at 0 eV. The state disperses through the Fermi energy at an angle of 14°. (**Inset**) Fermi surface calculated by Massida *et al.* (*21*). Open circles illustrate locations in the Brillouin zone at which spectra were taken; the closed circle marks the Fermi surface crossing.

R. J. Kelley, C. Quitmann, M. Onellion, Applied Superconductivity Center, University of Wisconsin, Madison, WI 53706, USA.
H. Berger, P. Almeras, G. Margaritondo, Institut de Physique Appliquée, École Polytechnique Fédérale, CH-1015 Lausanne, Switzerland.
*To whom correspondence should be addressed.

chrometer. The combined Gaussian energy resolution of the analyzer and the beamline was 15 to 25 meV as determined on a gold reference film. Fresh gold was periodically evaporated so that frequent calibrations of the Fermi energy E_F and resolution could be made. The angular resolution was ±1°.

Samples were transferred into the analysis vacuum chamber by way of a load lock chamber. This ensured that the samples were never baked, to avoid a loss of oxygen. The base pressure of the load lock chamber was 5×10^{-9} torr, and that of the main analysis chamber was 5×10^{-11} to 8×10^{-11} torr. Samples were loaded onto a cold finger and cleaved in situ at less than 40 K. We then performed LEED to test surface quality and orient the samples, which could be rotated about their surface normal in situ at low temperature. Orientations of ±1° were obtained. Temperature stability of ±1 K was obtained with a cryogenic temperature controller.

To determine the location of the Fermi surface, we used the criterion that the state has crossed the Fermi energy when a sudden decrease follows an intensity maximum. In data from an overdoped sample at 20 K (Fig. 1), a peak rapidly disperses between 8° and 14°, where it reaches a maximum. At 16° the peak is much reduced in intensity. In the superconducting state, this piling up of quasiparticle density of states persists past the Fermi level. A reduced feature can still be seen at 18° and even appears to be pulled back slightly from E_F. Here the Fermi level is between 14° and 16°. Use of a different angle would give an anomalous shift to the leading edge of the spectra, which could be mistaken for a larger gap value at say 18°.

Figure 2 shows data taken at the Fermi level crossing along the high-symmetry directions for an argon-annealed (underdoped) sample. The sizes of the gap, $\Delta_X(k_x = k_y) = 0 \pm 2$ meV and $\Delta_M = 17 \pm 2$ meV, were determined from the shift in the leading edge of spectra from the gold Fermi edge. This measurement is the most straightforward way to obtain a value for the gap. Other methods have been derived to fit a model function to the data. Values for the gap obtained by different methods were equally consistent (*2*). We adopted this method because we are primarily concerned with relative anisotropy changes rather than in absolute gap values. The results are consistent with previous photoemission results (*10*), which indicate a vanishing gap along the Γ-X direction (Fig. 2B). Photoemission resolution does not allow us to say that the gap along Γ-X is zero: The data indicate that $\Delta_X \leq 2$ meV. This low value has been interpreted as evidence for a $d_{x^2-y^2}$ symmetry superconductor (*10*).

The corresponding data for an oxygen-annealed (overdoped) sample (Fig. 3) indicate gap sizes of $\Delta_X = 10 \pm 2$ meV and $\Delta_M = 22 \pm 2$ meV. The value along the Γ-X direction is dramatically different from that of the underdoped sample (Fig. 3B). Note that for both Figs. 2A and 3A the gap along the Γ-M direction remains large (17 ± 2 and 22 ± 2 meV, respectively). The data indicate that overdoped samples exhibit an increase in the size of the gap along the Γ-X direction without significantly affecting the size of the gap along the Γ-M direction. The anisotropy between the Γ-X and Γ-M direction decreases with oxygen doping from $\Delta_M/\Delta_X = 20$ for underdoped samples to $\Delta_M/\Delta_X = 2.2$ for the oxygen-annealed crystal.

We took several precautions to avoid experimental artifacts. We reproduced the entire data set of Figs. 2 and 3 four times on different samples. We also checked parts of the data set (Fig. 2 or 3) an additional 11 times. Furthermore, we determined that the Fermi surface crossing in the Γ-X direction was the same, within 0.5°, for the two types of samples.

There was the possibility that the gap could have become more isotropic as a result of increased scattering. We performed several measurements on the two types of samples, including *ab*-plane and *c*-axis resistivity, transmission electron microscopy, *c*-axis supercurrent in applied magnetic field, and normal state angle-resolved photoemission. Some of these results have already been reported elsewhere (*18*). Earlier reports (*18*) indicate that the extrapolated residual *ab*-plane resistivity was lower for the samples with more oxygen. The results indicate that there is less scattering from overdoped samples and that the larger gap observed in the Γ-X direction for overdoped samples is not caused by increased scattering (*19*).

Ding *et al.* (*14*) suggested that their observation of a nonzero gap in the Γ-X di-

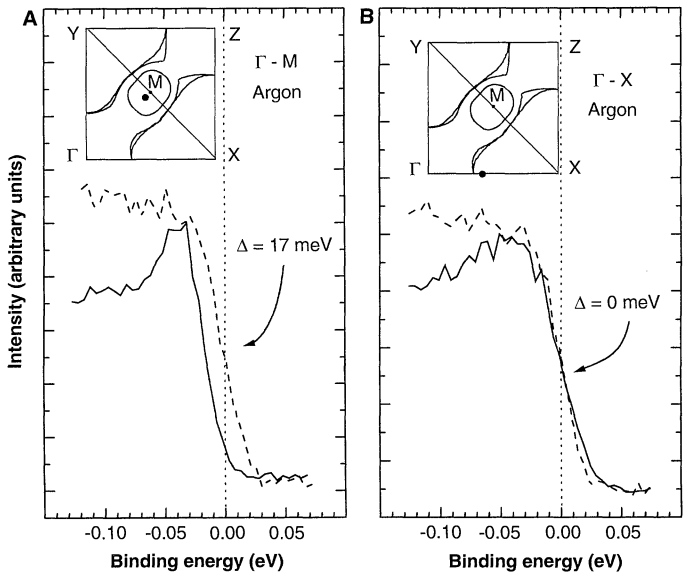

Fig. 2. Superconducting state angle-resolved photoemission spectra of an optimally doped (annealed in argon) sample with $T_c = 92$ K (sample temperature, 30 K; photon energy, 21 eV). (**A**) Spectrum taken at the Fermi surface along the Γ-M symmetry direction (solid line), and gold Fermi edge reference spectrum (dashed line). (**B**) Spectrum taken at the Fermi surface along the Γ-X symmetry direction (solid line), and gold Fermi edge reference spectrum (dashed line). (**Inset**) Fermi surface calculated by Massida *et al.* (*21*). The closed circle illustrates the location at which the superconducting state spectrum was taken.

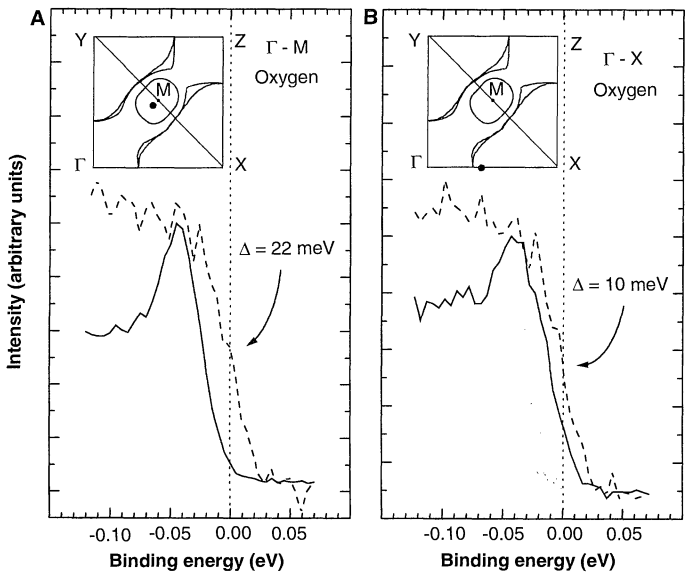

Fig. 3. Superconducting state angle-resolved photoemission spectra of an overdoped sample (annealed in oxygen) with $T_c = 83$ K (photon energy, 21 eV). (**A**) Spectrum taken at the Fermi surface along the Γ-M symmetry direction (solid line), and gold Fermi edge reference spectrum (dashed line). (**B**) Spectrum taken at the Fermi surface along the Γ-X symmetry direction (solid line), and gold Fermi edge reference spectrum (dashed line). (**Inset**) Fermi surface calculated by Massida *et al.* (*21*). The closed circle illustrates the location at which the superconducting state spectrum was taken.

rection was the result of the purely odd light-polarization symmetry of the normal state in this direction for their samples. As we reported earlier (*20*), and confirmed in this study, our normal state for overdoped samples is of mixed symmetry. Our observation of a nonzero gap along the Γ-X direction for overdoped samples thus seems an intrinsic effect attributable to doping.

Several important conclusions stem directly from our data. Because the gap along the Γ-X direction is nonzero for the overdoped samples, such samples cannot possess a pure $d_{x^2-y^2}$ superconducting order-parameter symmetry. However, the optimally doped and underdoped samples exhibit a very small gap in the Γ-X direction, small enough to be consistent with pure $d_{x^2-y^2}$ symmetry.

We considered several possible models in light of our data. The extended *s*-wave model proposed by Varma and co-workers (*15*) indicates that the gap nodes would appear at different Brillouin zone locations as the size of the Fermi surface changes. We observed no change in the Fermi wave vector in the Γ-X direction between the two types of samples, indicating that this part of the Fermi surface did not appreciably change its size. Given that the change in Fermi surface might be smaller than our experimental uncertainty, however, we can neither rule out nor explicitly support an extended *s*-wave model.

Our present data are consistent with an anisotropic *s*-wave order parameter. However, the gap must become more anisotropic for underdoped samples; this experimental result will constrain such theoretical models. The data are also consistent with a two-component order parameter (*2*), with the relative weights of the two components changing with stoichiometry (*3*–*5*). Such models (*3*–*5*) predict that the gap minima (or nodes) change location as the relative weight of the two components changes. There is the possibility that the nodes in the gap function shift with doping (*13*, *14*). Because we measured the gap only along the high-symmetry directions, we can neither confirm nor exclude this possibility.

In summary, we have reproducibly and reversibly changed the superconducting gap anisotropy from ~20:1 to ~2:1 by changing the oxygen doping. The data distinguish among some theoretical models and constrain other models. Our data provide a solution for the apparent conflict between earlier photoemission reports as to whether there is a zero in the gap along the Γ-X direction in the Brillouin zone.

REFERENCES AND NOTES

1. R. J. Kelley *et al.*, *Phys. Rev. B* **50**, 590 (1994).
2. J. Ma *et al.*, *Science* **267**, 862 (1995).
3. J. Betouras and R. Joynt, *Europhys. Lett.* **31**, 119 (1995).
4. Q. P. Li *et al.*, *Phys. Rev. B* **48**, 437 (1993).
5. G. Kotliar, *ibid.* **37**, 3664 (1988).
6. S. D. Adrian *et al.*, *ibid.* **51**, 6800 (1995); A. G. Sun *et al.*, *Phys. Rev. Lett.* **72**, 2267 (1994); J. Buan *et al.*, *ibid.*, p. 2632.
7. D. A. Wollman *et al.*, *Phys. Rev. Lett.* **71**, 331 (1993).
8. W. N. Hardy *et al.*, *ibid.* **70**, 3999 (1993).
9. C. C. Tsuei *et al.*, *ibid.* **73**, 593 (1994).
10. Z.-X. Shen *et al.*, *ibid.* **70**, 1553 (1993).
11. The interpretation of (*10*) has been criticized by, for example, G. D. Mahan [*ibid.* **71**, 4277 (1993)].
12. R. J. Kelley *et al.*, *ibid.*, p. 4051.
13. H. Ding *et al.*, *ibid.* **74**, 2784 (1995).
14. H. Ding *et al.*, *ibid.* **75**, 1425 (1995).
15. C. M. Varma *et al.*, *ibid.* **63**, 1996 (1989); *ibid.* **64**, 497 (1990).
16. K. A. Müller, *Nature* **377**, 133 (1995).
17. P. D. Han and D. A. Payne, *J. Cryst. Growth* **104**, 201 (1990).
18. C. Kendziora *et al.*, *Physica C*, in press.
19. R. Fehrenbacher and M. R. Norman, *Phys. Rev. B* **50**, 3495 (1994); *Physica C* **235**, 2407 (1995).
20. J. Ma *et al.*, *Phys. Rev. B* **51**, 9271 (1995).
21. S. Massida *et al.*, *Phys. Lett. A* **122**, 197 (1987).

22. We benefited from conversations with I. Bozovic, J. Eckstein, R. Joynt, A. Chubukov, G. Varelogiannis, and V. Kresin. The staff at the Wisconsin Synchrotron Radiation Center (SRC), particularly R. Hansen and T. Baraniak, were most helpful. Financial support was provided by the U.S. National Science Foundation, both directly and through support of the SRC, École Polytechnique Fédérale Lausanne, Fonds National Suisse de la Recherche Scientifique, and the Deutsche Forschungsgemeinschaft.

28 July 1995; accepted 1 December 1995

Model Estimations Biased by Truncated Expansions: Possible Artifacts in Seismic Tomography

Jeannot Trampert* and Roel Snieder

In most linear imaging problems, where the model to be sought is expanded in a set of basis functions, it is common practice to truncate the set at a certain (arbitrary) level. The solution then depends on the chosen parameterization, and neglected basis functions may leak into the solution to produce artifacts in the retrieved model. An unbiased estimate of the coefficients of the true model may be obtained in the chosen finite basis set; here, a method to suppress leakage is illustrated on an example of global seismic tomography.

A linear inverse problem is defined as one in which the data are linear functionals of the model. Specifically, a datum, d_i, is related to the unknown model $m(\mathbf{r})$ by

$$d_i = \int G_i(\mathbf{r}) m(\mathbf{r}) d\mathbf{r} \qquad (1)$$

where $G_i(\mathbf{r})$ represents the known data kernels derived from theory. There are many ways of inferring models from data (*1*, *2*). We have restricted our discussion here to the convenient case where the model to be sought is expanded in a complete set of basis functions B_j such that

$$m(\mathbf{r}) = \sum_{j=1}^{\infty} c_j B_j(\mathbf{r}) \qquad (2)$$

Such an approach applies to a large class of interpolation, spectral analysis, and imaging problems in astronomy, geophysics, and medicine. Many different parameterizations (choices of basis functions) are possible, but as long as the chosen set is complete, they are all equivalent. To describe the model fully, the set of basis functions must be complete, and hence the summation in Eq. 2 has to be carried out to infinity. This would lead to an ill-posed inverse problem. In practice, we are limited by the finite resolution of the data, so that we have to choose an upper limit, L, for the expansion. This leads to a classical linear inverse problem for L coefficients, c_j, which may be represented by the matrix equation

$$\mathbf{d} = \mathbf{A}\mathbf{c} \qquad (3)$$

where the matrix $\mathbf{A}$ is defined by $A_{ij} = \int G_i(\mathbf{r}) B_j(\mathbf{r}) d\mathbf{r}$. The truncation of the expansion leads to a smoothed estimation of the true model, regardless of the real smoothness properties of the true model. Generally, we have no precise a priori knowledge of the unknown function $m(\mathbf{r})$, and our choice of L is guided by technical questions, such as the size of the inverse problem. Any real structure unrepresented by the finite number of basis functions fixed by L may produce a bias in our estimate of the low-order expansion of the true model.

We will show here that leakage may occur from neglected basis functions to the finite number of estimated coefficients and that inhomogeneous model sampling is responsible for this bias (*3*, *4*). We are thus confronted with the undesirable property that the model depends on the way it is sampled. We present here a mathematical formulation that takes the complete unknown model structure into account and suppresses leakage with the use of a weighted least-squares algorithm. The weighting ma-

J. Trampert, Ecole et Observatoire de Physique du Globe, URA 1358 ULP-CNRS, 5 Rue René Descartes, 67084 Strasbourg Cedex, France.
R. Snieder, Department of Theoretical Geophysics, University of Utrecht, P.O. Box 80.021, 3508 TA Utrecht, Netherlands.

*To whom correspondence should be addressed.